AER/AGS Open File Report 2019-03

Alberta Energy Regulator

3D Property Modelling of the Bedrock Hydrostratigraphy in the Fox Creek Area, West-Central Alberta

AGS
ALBERTA GEOLOGICAL SURVEY

AER/AGS Open File Report 2019-03

3D Property Modelling of the Bedrock Hydrostratigraphy in the Fox Creek Area, West-Central Alberta

M. Babakhani, S. Mei, L.A. Atkinson and B.D. Smerdon

Alberta Energy Regulator
Alberta Geological Survey

August 2019

ISBN 978-1-4601-3990-5

If you use information from this publication in other publications or presentations, please acknowledge the AER/AGS. We recommend the following reference format:

Babakhani, M., Mei, S., Atkinson, L.A. and Smerdon, B.D. (2019): 3D property modelling of the bedrock hydrostratigraphy in the Fox Creek area, west-central Alberta; Alberta Energy Regulator / Alberta Geological Survey, AER/AGS Open File Report 2019-03, 19 p.

Publications in this series have undergone only limited review and are released essentially as submitted by the author.

Published August 2019 by:
Alberta Energy Regulator
Alberta Geological Survey
4th Floor, Twin Atria Building
4999 – 98th Avenue
Edmonton, AB T6B 2X3
Canada

Tel: 780.638.4491
Fax: 780.422.1459
Email: AGS-Info@aer.ca
Website: www.ags.aer.ca

Contents

Tables

Figures

Acknowledgements

The authors wish to acknowledge the following individuals for their contributions to this report:

- L.D. Andriashek (AGS) for his helpful and ongoing discussion about groundwater resources within the Paskapoo Formation and comments on an earlier version of this report, and
- S. Lyster and K.E. MacCormack (AGS) for reviewing an earlier version of this report.

Abstract

To aid hydrogeological conceptualization, a three-dimensional (3D) model of sandstone abundance was developed for the Upper Cretaceous–Paleogene bedrock deposits in the vicinity of the Town of Fox Creek, Alberta. Sandstone abundance was derived from a combination of gamma-ray logs and water well lithological descriptions, and presented as the net sandstone to gross interval thickness (referred to as net-to-gross ratio: NGR). The NGR data were simulated in 3D for a 22 170 km^2 area through a series of 10 stacked submodel domains from the top of First White Speckled Shale unit (Wapiabi Formation) to the present-day bedrock topographic surface. This interval includes the Lea Park, Wapiti, Battle, Scollard, and Paskapoo formations and is up to about 1800 m in depth. The model was created in Schlumberger Limited’s Petrel 2015 software platform and would be appropriate for regional-scale assessments (1:100 000) rather than site-specific investigations. The 3D property model illustrates the degree of heterogeneity of sandstone abundance in the bedrock, which can be used to conceptualize the hydrostratigraphy assuming that the NGR values are a proxy for permeability. Several trends that have hydrogeological implications within the study area emerge as a result of 3D property modelling, including a nearly continuous and approximately 230 m thick sandstone unit in the basal portion of the undifferentiated Wapiti Formation; the absence of a basal sandstone unit within the Paskapoo Formation; confirmation of abundant but highly heterogeneous sandstone in the uppermost portion of the Paskapoo Formation; and a general dominance of NGR values of about 0.4 for the Upper Cretaceous–Paleogene bedrock deposits. The 3D property model of the study area offers new insight into the distribution of aquifers and aquitards within the Upper Cretaceous–Paleogene bedrock deposits.

1 Introduction

The region centred on the Town of Fox Creek, Alberta, has experienced an increase in water use since 2012 because of exploration and development of the liquid-rich shale gas plays in the Duvernay and Montney formations (Alberta Energy Regulator, 2019). Compared to surface water, groundwater is an increasingly important alternative source of water in this region. The greatest potential for shallow groundwater availability is the uppermost bedrock formations, primarily sandstone bodies within the Paskapoo and Wapiti formations. In an effort to better understand the hydrogeological conditions of the area, the Alberta Geological Survey (AGS) completed a regional-scale hydrogeological characterization project in the vicinity of the Town of Fox Creek, Alberta.

A major component of the hydrogeological characterization project was the development of a regional hydrostratigraphic model to identify subsurface zones of similar lithology. For the Paleogene−Quaternary sediments, a three-dimensional (3D) model was described by Atkinson and Hartman (2017); whereas the objective of the current report is to document a 3D model of the bedrock hydrostratigraphy. The bedrock hydrostratigraphy is characterized by the abundance of sandstone determined from a combination of oil- and gas-well geophysical logs, and lithological logs from water wells. The 3D renderings of the subsurface enhance the conceptualization of hydrostratigraphy in the Fox Creek area at a scale appropriate for assessing nonsaline groundwater circulation. The data will also help to better understand the degree of heterogeneity associated with the bedrock formations.

1.1 Study Area

The study area is 22 170 km^2 and centred on the Town of Fox Creek (Figure 1), which is located approximately 260 km northwest of Edmonton. The boundary of the study area was defined by hydrological features (i.e., sub-basin drainage boundaries) within the Peace River and Athabasca River basins and the Cordilleran deformation belt (Figure 1). This hydrologically defined study area is nested within a slightly larger study area defined for a 3D geological model of west-central Alberta (Babakhani and MacCormack, 2019; Corlett et al., 2019). Within the 3D geological model, 49 geological surfaces and 4 unconformities (sub-Permian, sub-Triassic, sub-Jurassic, sub-Cretaceous unconformities) between the Precambrian basement and the present-day bedrock topographic surface were created.

For the purpose of developing a regional hydrostratigraphic model, the bedrock units from the top of First White Speckled Shale unit (Wapiabi Formation) to the bedrock topographic surface were considered. This interval includes the Lea Park, Wapiti, Battle, Scollard, and Paskapoo formations (Figure 2).

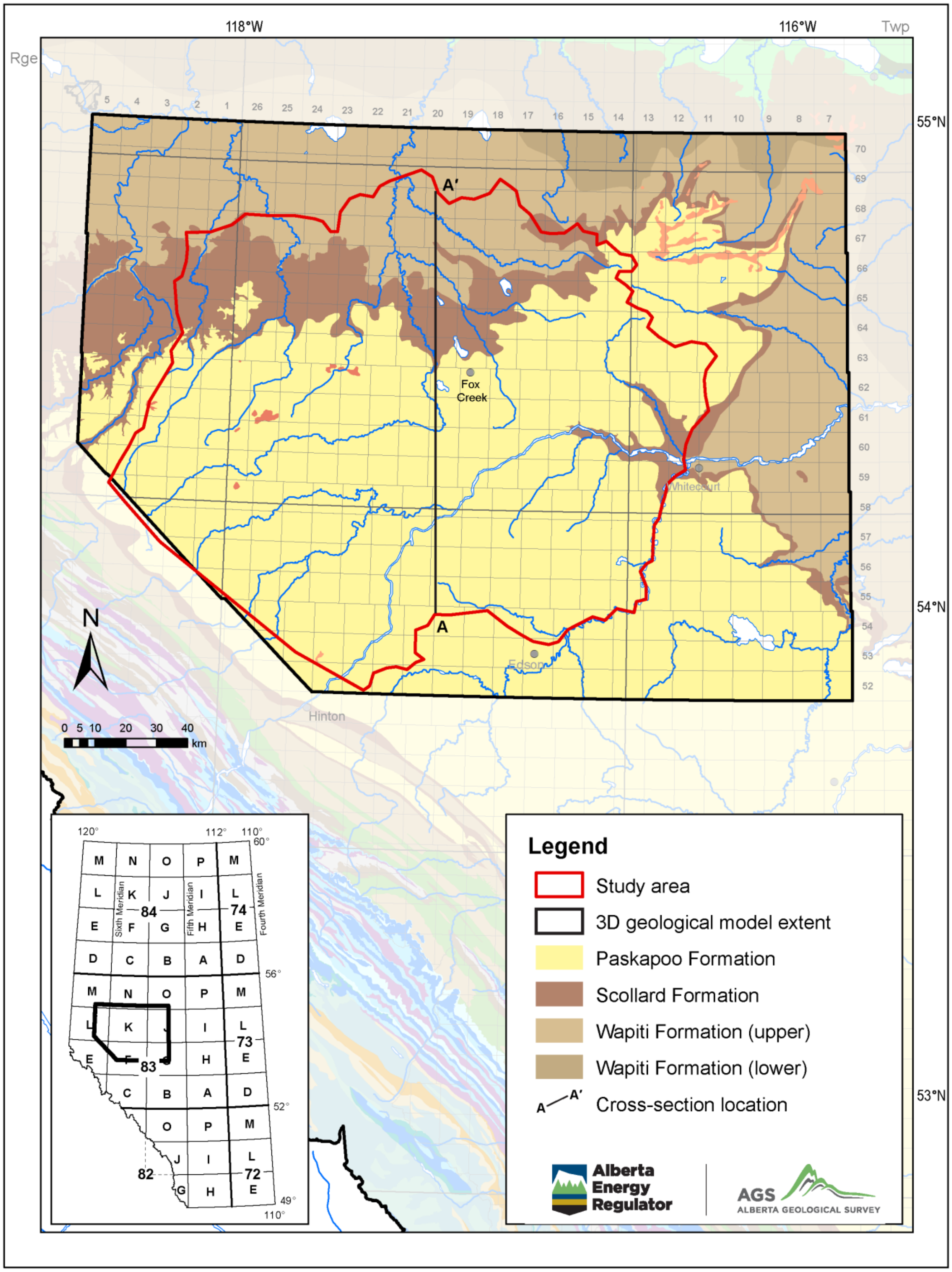

Figure 1. Location and bedrock geology map of the study area (Prior et al., 2013). Inset map of Alberta shows the extent of the three-dimensional (3D) geological model by Babakhani and MacCormack (2019) and Corlett et al. (2019).

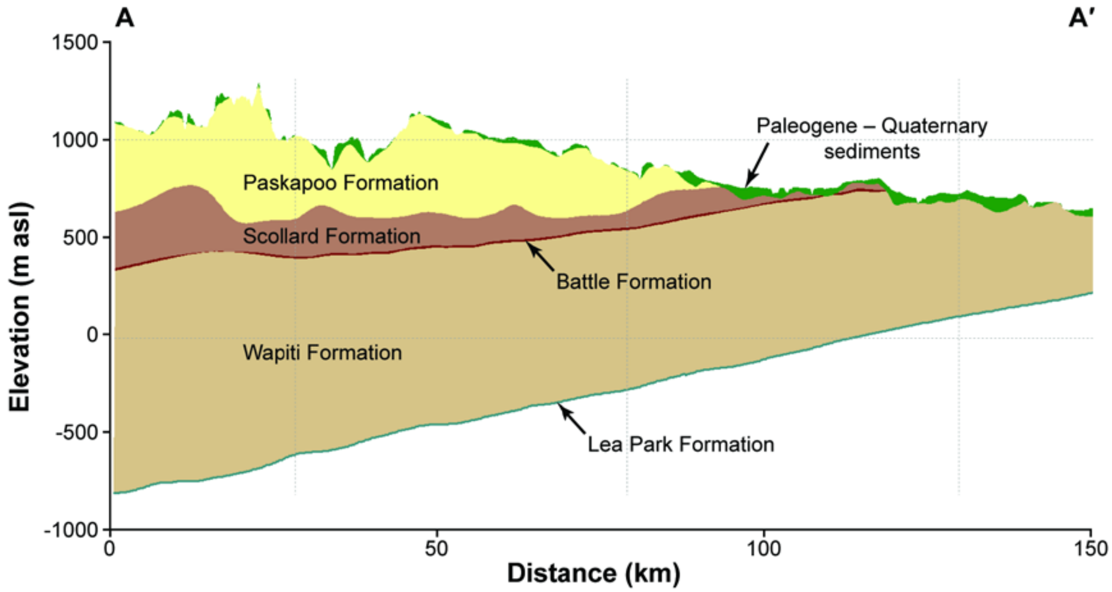

Figure 2. Simplified geological cross-section for A–A′ (shown in Figure 1), illustrating the wedge-shaped geometry of the bedrock formations overlying the Lea Park Formation.

2 Methods

The approach used in this study builds on the slice mapping methodology described in Parks and Andriashek (2009) and Atkinson et al. (2017). The methodology involves partitioning the subsurface into a series of slices and evaluating sandstone abundance for each slice, then grouping several slices and simulating the sandstone abundance in 3D using geostatistical methods. The groupings of slices are then stacked to represent a complete 3D hydrostratigraphic model for the study area. The approach used in this study attempts to balance incorporating varying degrees of subsurface heterogeneity from available data. The desired outcome was to capture a 'medium' degree of heterogeneity (Figure 3; Tyler and Finley, 1991) that would meet the needs of hydrogeological characterization in this region. More detailed 3D modelling of subsurface properties could be achieved by upscaling directly from the source data (e.g., continuous well log data).

Sandstone abundance is described as the net sandstone to gross interval thickness (referred to in this report as net-to-gross ratio: NGR) that was derived from gamma-ray logs. A gamma-ray log shows a record of measurement of the natural emission of gamma rays in the rocks surrounding the logging tool within a borehole. The most common sources of natural gamma rays are potassium, thorium, and uranium, which are typically found in clay-rich clastic rocks. As a result, gamma-ray logs are commonly used to describe a sandstone–shale sequence because shale contains a high proportion of clays (producing a high gamma-ray value) whereas clean sandstone does not (producing a low gamma-ray value). In this study, the hydrostratigraphic model was developed by identifying sandstone-rich bodies within a sandstone–siltstone–shale sequence.

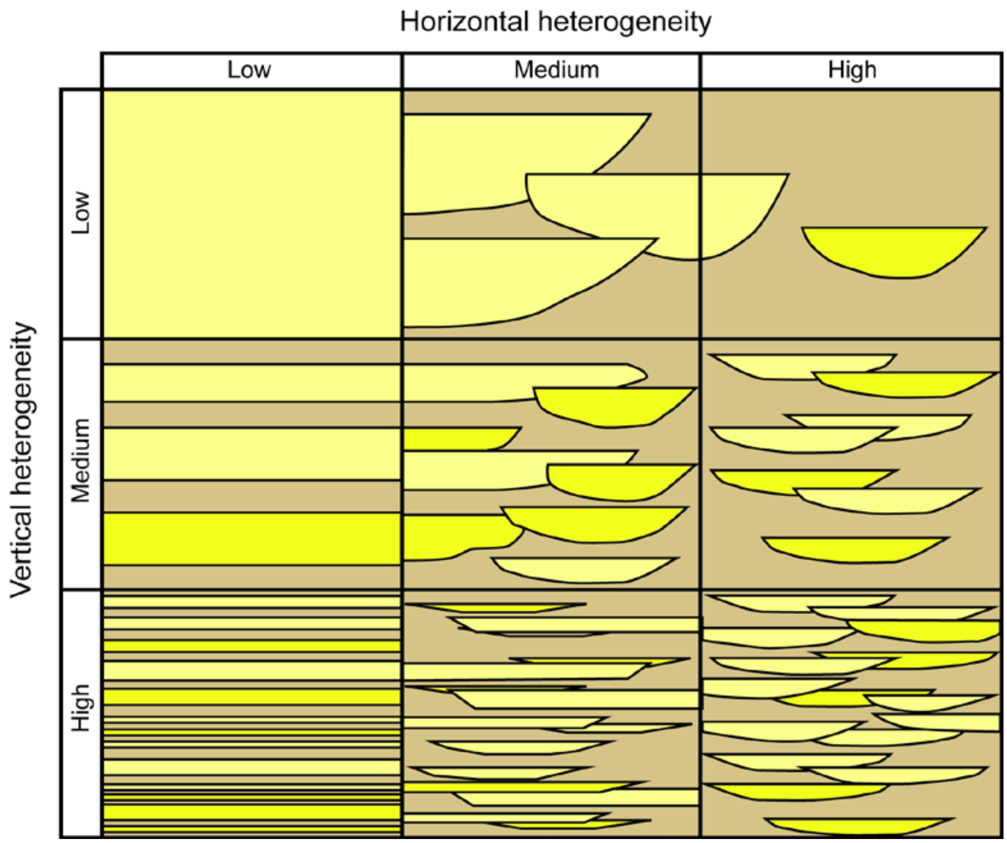

Figure 3. Conceptual representation of subsurface heterogeneity considered during property modelling (adapted from Tyler and Finley, 1991). The slice mapping approach used in this study represents a 'medium' degree of vertical and horizontal heterogeneity.

2.1 Data and Sources of Error

2.1.1 Slice Mapping

The subsurface was partitioned into a series of slices constrained to three distinct geological surfaces: i) the top of the First White Speckled Shale unit of the Wapiabi Formation; ii) the top of Battle Formation; and iii) the bedrock topographic surface. The rationale for generating slices between these surfaces was to ensure that sediments of approximately the same time interval (i.e., in a slice) were maintained in partitioning gamma-ray log measurements and calculating resultant NGR values.

The First White Speckled Shale unit is composed of a calcareous mudstone with bentonite, fish remains, nodular phosphate, and concretions of siderite and calcite (Leckie et al., 1994). It can be recognized by high deflections/spikes on gamma-ray logs due to its high radioactive uranium content associated with abundant kerogen and bentonite deposited in the shale. To generate a surface of the First White Speckled Shale unit in this study, 39 748 stratigraphic picks were used from AccuMap™ (IHS Markit, 2018) and internal Alberta Energy Regulator / Alberta Geological Survey (AER/AGS) oil and gas well data holdings, as well as picks made by the AGS specifically for this study to infill and refine the generated surface.

The Battle Formation is an important stratigraphic marker (Elliott, 1960) and regional aquitard in the nonmarine Upper Cretaceous succession across a wide area of west-central Alberta. The Battle Formation has a generally high gamma-ray signature and a characteristically low resistivity signature, which is usually the best guide to its position. The upper and lower contacts are best picked at the sharp upward deflections to the left (base of the Battle Formation) and right (top of the formation) on neutron, density, and sonic curves, ideally in combination with similar deflections on a resistivity log (Hathway, 2011a, b). In some areas, the Battle Formation thins or has been completely removed by erosion at the base of the Scollard Formation (Hathway, 2011a, b). To generate a surface of the Battle Formation, 3739 stratigraphic picks were used from AccuMap and internal AER/AGS oil- and gas-well data holdings.

There are several sources of error associated with creating geological surfaces from borehole data. A brief summary is provided here:

- confusion of the true vertical depth with the measured depth of picks for deviated wells when deviation survey data are missing,
- potential error of the elevation of picks due to inaccurate reference elevation (i.e., kelly bushing),
- human error associated with inconsistent or incorrect placement of the pick on the well logs, and
- error in well log depth calibration and entry.

These errors can be minimized to obtain a high accuracy for the reference horizons, which in turn ensures that the data for each slice represents the equal time intervals. The iterative culling process is described in Mei (2009).

2.1.2 Borehole Logs

The digital logs used in this study include gamma-ray logs from 19 139 oil and gas wells including both open and cased boreholes, and lithological descriptions derived from lithological/hydrogeological information from 3690 water wells in the Alberta Water Well Information Database (AWWID; Alberta Environment and Parks, 2018).

The gamma-ray log measures the natural gamma-ray emissions from radioactive formations. Since many gamma rays can pass through steel casing, the log can be recorded in both open and cased holes. Radiation is naturally erratic and the measured gamma-ray values can be characterized by statistical variation. The gamma-ray value can be affected by i) radiation intensity of the formation; ii) the efficiency of the radiation counter; iii) borehole logging speed; and iv) the borehole environment (e.g., sonde position within the borehole, borehole size, mud weight, casing size and weight, and cement thickness). As a result, gamma-ray tool calibration and environment correction are commonly applied after logging. Error may be introduced in any step during logging and calibration.

The AWWID has several potential sources of error, including i) geographic position inaccuracy and ii) inconsistency and error in describing and recoding water well lithology by different water well contractors. For geographic position, many water wells are not formally surveyed and arbitrarily located to the centroid of a quarter-section on the Alberta Township Survey grid. As a result, colocation of wells is often encountered in the AWWID, which required further examination and screening.

2.2 Determining Sandstone Abundance

Sandstone abundance, as described by the net-to-gross ratio (NGR) of sandstone, was determined following a series of steps to normalize borehole log data and assign values to subsurface slices. The workflow used in this study is shown in Figure 4, including data assembly, NGR determination, and 3D property modelling.

2.2.1 Borehole Log Processing

The gamma-ray logs used include both open-hole and cased-hole logs. The through-casing gamma-ray logs are attenuated by the casing and, thus, need to be corrected to make them consistent with the open-hole logs below the casing. This is carried out by log normalization using the reference statistics derived from the open-hole gamma-ray logs below the casing. This removes the bias caused only by the surface casing and makes the normalized through-casing gamma-ray log consistent with the log from the open-hole portion below the casing. Then, the normalized through-casing gamma-ray log and the log from the open-hole portion below the casing are merged as a single well path. The method described by Quartero et al. (2014) is used only when the log from the open-hole portion is not usable or unavailable. In addition, normalization is also used to correct biased, attenuated, or erroneous gamma-ray logs caused by various reasons other than surface casing. Anomalous logs were first identified as those that have a median gamma-ray value of <50 American Petroleum Institute (API) units or >100 API. As a result, 2122 anomalous logs were identified and corrected by log normalization using reference statistics obtained from all other logs for the interval of interest. For final use, all logs were despiked using a low threshold of 6 API and a high threshold of 250 API, based on examination of the log statistics.

The lithological descriptions of water wells recorded by water well contractors were examined, classified, coded, and grouped into two categories: i) sand/sandstone and ii) mud/shale. Available gamma-ray and resistivity logs collected from water wells were used to validate the water well sediment descriptions. The AWWID well locations were modified if property information (e.g., lot area) was found on the original well records. Elevation of water wells were extracted from a light detection and ranging (LiDAR) elevation model to ensure that each borehole was projected on a cross-section at the appropriate elevation. Wells with duplicate locations were evaluated on cross-section with the surrounding data and the accuracy of lithology information contained within the record, and the water wells identified with the most correct lithological description were kept for analysis.

The binary coding (sand/sandstone or mud/shale) of the lithology of water wells were converted into pseudo gamma-ray logs by arbitrarily assigning the sandstone code a 5 API value and the mud/shale a 120 API value. This arbitrary assignment was intended to identify the distribution trend of porous/nonporous rock units by calculating the NGR of the porous rock unit (e.g., sandstone), and the particular gamma-ray value is not of direct interest. The binary-coded water well data were then merged with the oil and gas well data for NGR calculations.

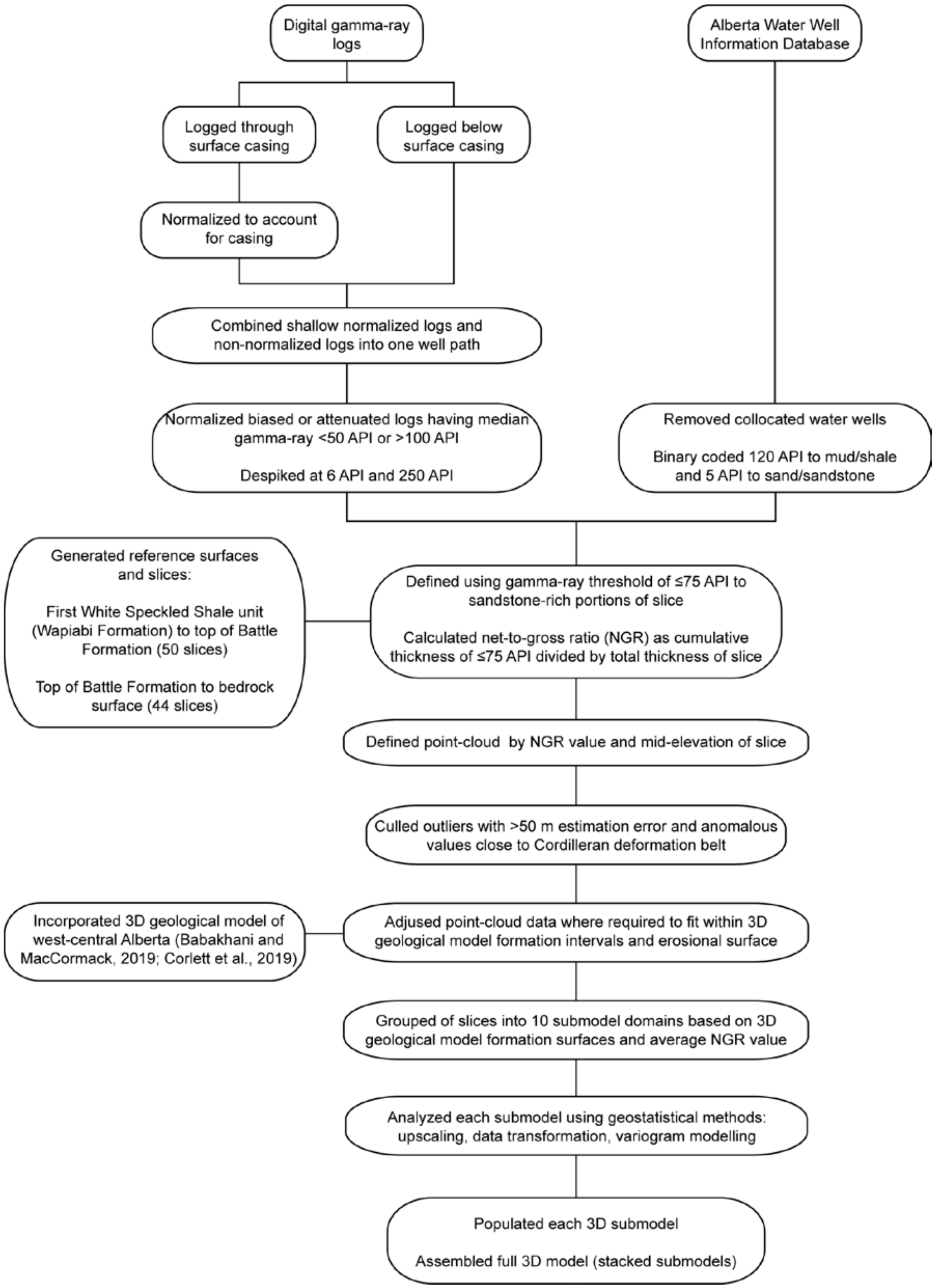

Figure 4. Workflow diagram for the net-to-gross determination and three-dimensional (3D) property modelling.

2.2.2 Calculation of Net-to-Gross Ratio

To capture a medium degree of heterogeneity (Figure 3), the net-to-gross ratio was calculated using gamma-ray values from borehole logs for each subsurface slice. Effectively, this slice-mapping approach resulted in upscaling knowledge of sandstone abundance to slices that represent time intervals of similar sediment deposition.

The interval between the top of the First White Speckled Shale unit of the Wapiabi Formation and the top of the Battle Formation was partitioned into 50 slices of variable thickness. The interval between the top of the Battle Formation and the bedrock topographic surface was partitioned into 44 slices of variable thickness. In total, 94 slices were made for the interval including, in ascending order, the Lea Park, Wapiti, Battle, Scollard, and Paskapoo formations.

The merged borehole dataset was assigned a threshold gamma-ray value of ≤75 API to define the sandstone-rich portions for each well in a slice. The NGR was calculated by dividing the cumulative thickness of the sandstone-rich portions by the gross or total thickness of each slice. The result is layers of NGR values that represent a point-cloud dataset with x, y, and z coordinates for the midpoint of each slice for a given borehole location, and the associated NGR values for the bedrock formations (Figure 5).

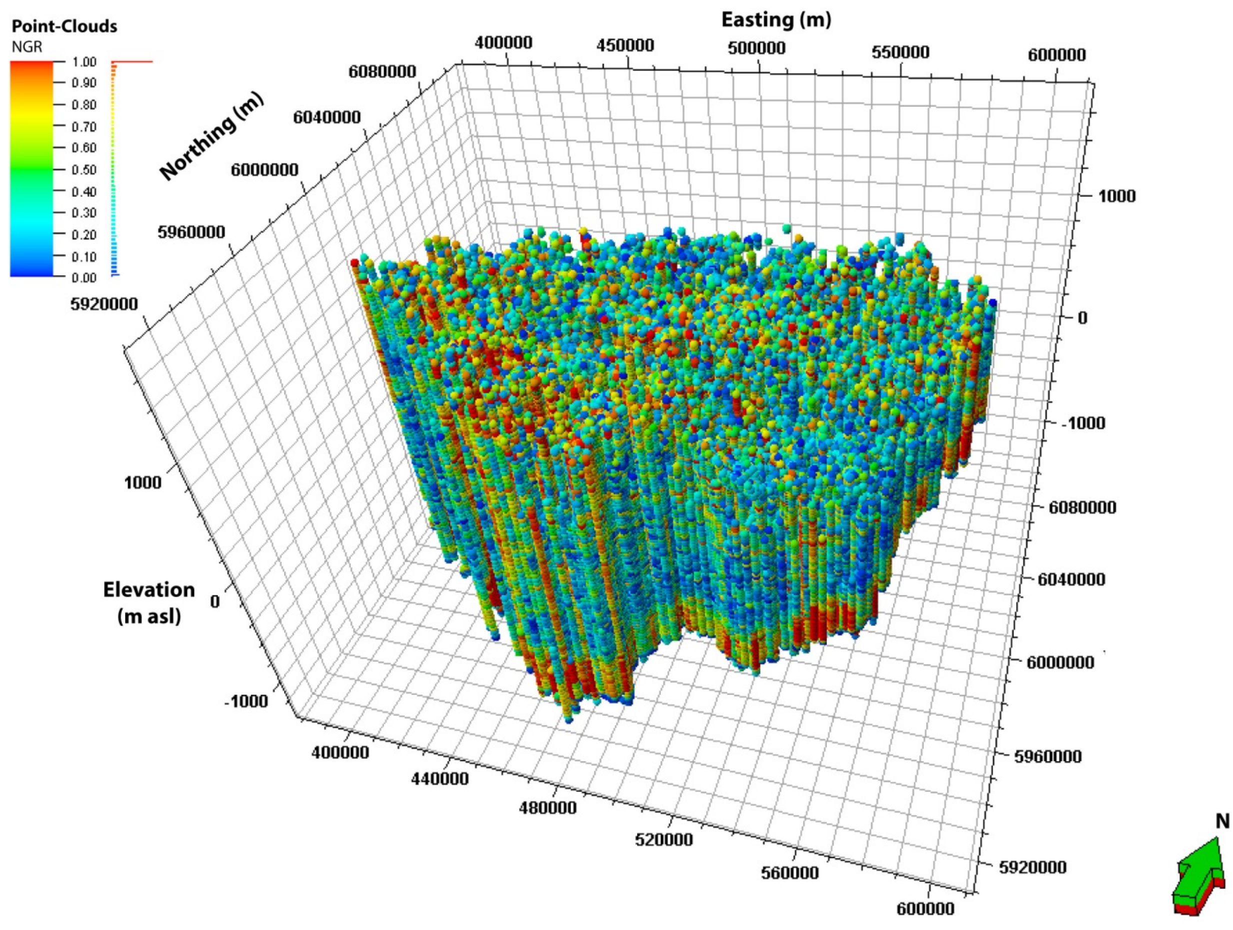

Figure 5. Point-cloud of net-to-gross ratio (NGR) values from the bedrock surface to the top of the First White Speckled Shale unit of the Wapiabi Formation.

2.3 Alignment to the Geological Model

Prior to simulating NGR values in 3D space, the point-cloud dataset underwent minor culling and adjustment to align with the 3D geological model of west-central Alberta (Babakhani and MacCormack, 2019; Corlett et al., 2019) and updated bedrock topographic surface for the Fox Creek area (Atkinson and Hartman, 2017), both of which were developed concurrently with the point-cloud NGR data. The 3D geological model had slightly different surfaces representing sliced surfaces defined in Section 2.1.1.

Each slice was evaluated to detect any outliers of extremely high or low values. The outliers in this step refer to any data values that have an estimation error >50 m at each data location and anomalous data located close to the Cordilleran deformation belt. For each slice, the point-cloud NGR data were detrended and interpolated using ordinary kriging. The difference between each NGR value and the interpolated surface were compared, and any NGR values with an estimation error >50 m were removed. After culling the outliers from each slice, the final dataset were imported into Schlumberger Limited's Petrel 2015 software platform for further evaluation and modelling.

To account for the difference between the surfaces defined for slice mapping and equivalent formation top surfaces developed in the 3D geological model of west-central Alberta, some adjustment of the point-cloud data was required. The formation surfaces from the 3D geological model were prioritized, and NGR values from slices in close proximity to formation boundaries were reallocated to the appropriate slice. For example, consider the interval from the top of the Battle Formation to the top of the Scollard Formation. Some portions of the slices representing this interval (and the resultant NGR data) were below the top of the Battle Formation and some were above the top of the Scollard Formation. Data occurring below the top of the Battle Formation were allocated to the underlying Wapiti Formation, and data occurring above the top of the Scollard Formation were allocated to the Paskapoo Formation.

The erosional surface of the bedrock topography is a unique surface that also required some of the slice data to be adjusted. For simplicity, any NGR values that were above the bedrock topographic surface were removed.

2.4 3D Property Modelling

Property modelling allows the distribution of an attribute between data locations by various methods of estimation or simulation. Petrophysical modelling in Petrel was used to interpolate and estimate continuous NGR values for the study area. To develop a 3D property model of the bedrock hydrostratigraphy, the NGR data were simulated in 3D for a series of 10 stacked submodel domains, where each NGR submodel was simulated independently.

2.4.1 Submodel Domains

The submodel domains were defined based on formations surfaces from the 3D geological model of west-central Alberta (Figure 6) and apparent vertical trend in the average sandstone abundance (Figure 7). For each submodel, a 500 by 500 m grid cell size was defined in Petrel using the simple grid tool. Table 1 summarizes the 10 submodel domains and NGR values within the associated slices.

2.4.2 Geostatistical Analysis

Simulating properties in 3D requires geostatistical analysis having multiple steps, including upscaling and transforming the data, defining a variogram through modelling, and finally populating the 3D model. Typically within Petrel, point-cloud data would be scaled up to the 3D modelling grid. Because the NGR values were calculated for slices in this study, the NGR values (mid-elevation of a slice) were scaled up to the cells of the simple grid in which they occur. Variograms were used to quantify the spatial structure of the NGR values, and transformations were used to populate the 3D model.

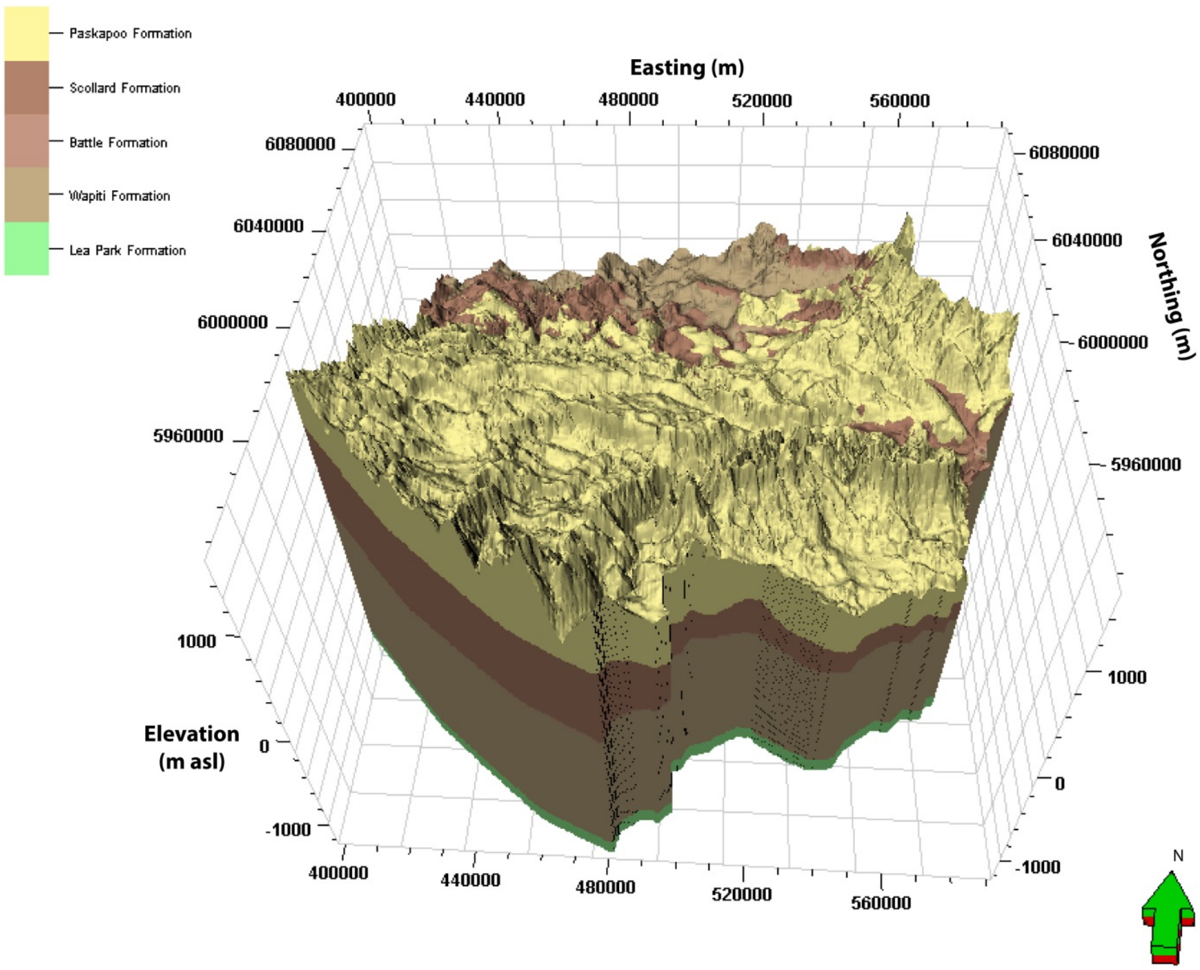

Figure 6. Formations within the study area, from the three-dimensional (3D) geological model (Babakhani and MacCormack, 2019; Corlett et al., 2019).

The NGR values in most of the slices have a highly skewed distribution, which makes populating the 3D model more challenging. Normal score transformation was applied on the upscaled NGR values to reduce the impact of the high values on variogram modelling. Normal score transformation makes the data stationary with a mean of zero and standard deviation of one and a normal distribution. Normal distribution has some useful mathematical features that are useful in modelling based on the geostatistical analysis.

The spatial structure of each submodel is defined by variogram modelling. A three-structure spherical variogram model was needed to fit the experimental variogram in horizontal (major and minor) and vertical directions. The settings for each submodel are unique because of the different spatial variability in each group of slices. Table 2 summarizes the variogram settings for each submodel domain.

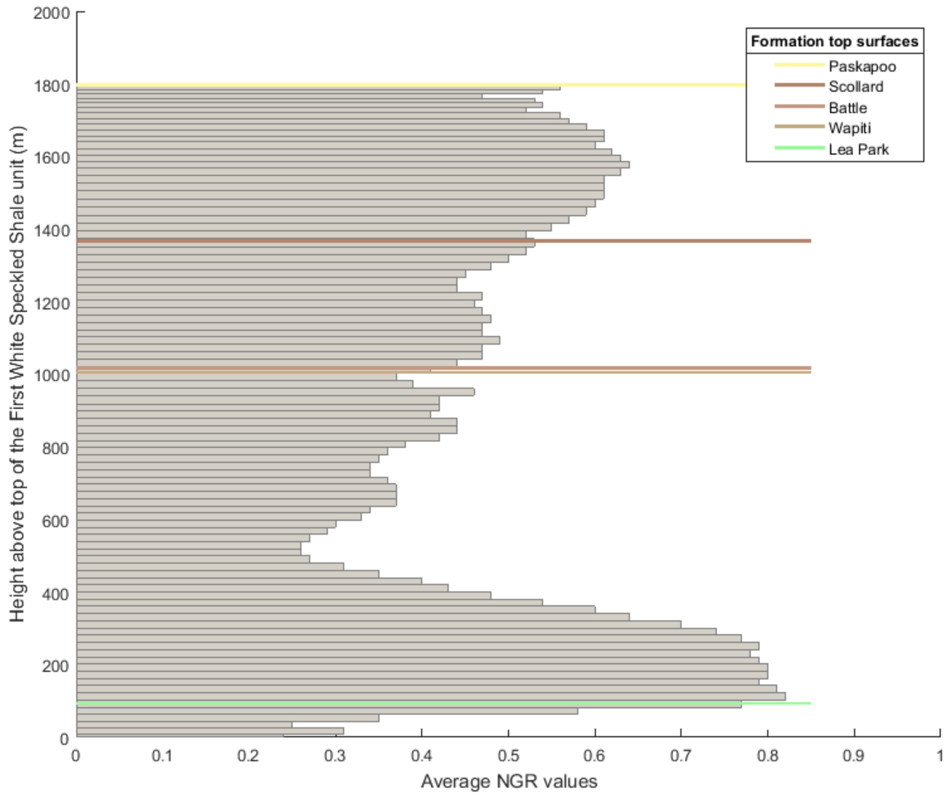

Figure 7. Average sandstone abundance per slice, from the First White Speckled Shale unit of the Wapiabi Formation to the bedrock topographic surface. Abbreviation: NGR, net-to-gross ratio.

Table 1. Summary of submodel domains. Abbreviation: NGR, net-to-gross ratio.

Submodel	Geological Interval	NGR Slices	Average NGR Value
1	Lea Park Formation – lower portion	1–3	0.12
2	Lea Park Formation – upper portion	4–5	0.39
3	Wapiti Formation 1 (basal sand)	6–17	0.86
4	Wapiti Formation 2	18–23	0.54
5	Wapiti Formation 3	24–33	0.23
6	Wapiti Formation 4	34–42	0.30
7	Wapiti Formation 5	43–45	0.38
8	Battle Formation	46–56	0.32
9	Scollard Formation	57–80	0.42
10	Scollard Formation to bedrock topographic surface, including the Paskapoo Formation	81–94	0.50

Table 2. Summary of variogram parameters for each submodel domain.

Submodel	Geological Interval	Structure	Type	Sill	Major Range (m)	Minor Range (m)	Vertical Range (m)
1	Lea Park Formation –	0	Nugget	0.8			
	lower portion	1	Spherical	0.05	26 700	24 000	8
		2	Spherical	0.15	80 000	61 200	13
2	Lea Park Formation –	0	Nugget	0.77			
	upper portion	1	Spherical	0.04	45 000	44 000	10
		2	Spherical	0.19	126 000	121 000	40
3	Wapiti Formation 1	0	Nugget	0.8			
	(basal sand)	1	Spherical	0.06	36 100	36 000	120
		2	Spherical	0.14	92 000	82 000	240
4	Wapiti Formation 2	0	Nugget	0.66			
		1	Spherical	0.04	41 450	33 500	40
		2	Spherical	0.3	135 000	101 600	150
5	Wapiti Formation 3	0	Nugget	0.8			
		1	Spherical	0.05	43 000	43 000	100
		2	Spherical	0.15	90 000	87 000	200
6	Wapiti Formation 4	0	Nugget	0.8			
		1	Spherical	0.08	40 000	40 000	70
		2	Spherical	0.12	113 000	82 000	180
7	Wapiti Formation 5	0	Nugget	0.8			
		1	Spherical	0.08	36 000	35 000	100
		2	Spherical	0.12	100 000	90 000	200
8	Battle Formation	0	Nugget	0.8			
		1	Spherical	0.08	55 500	33 400	25
		2	Spherical	0.12	85 900	82 800	50
9	Scollard Formation	0	Nugget	0.79			
		1	Spherical	0.08	22 000	21 500	90
		2	Spherical	0.13	93 000	86 000	250
10	Scollard Formation to bedrock topographic surface, including the Paskapoo Formation	0	Nugget	0.64			
		1	Spherical	0.17	17 000	8000	130
		2	Spherical	0.19	140 000	10 000	300

2.4.3 Populating the 3D Model

Simple kriging was the estimation method used for property modelling in this study. Kriging uses the variogram of each submodel to weight the available data and estimate the values at unsampled locations using the available data. The property model of the NGR values is populated by a back transform to the original distribution of the data. The final result is a series of stacked submodels that depict the sandstone abundance of the bedrock deposits (Figure 8).

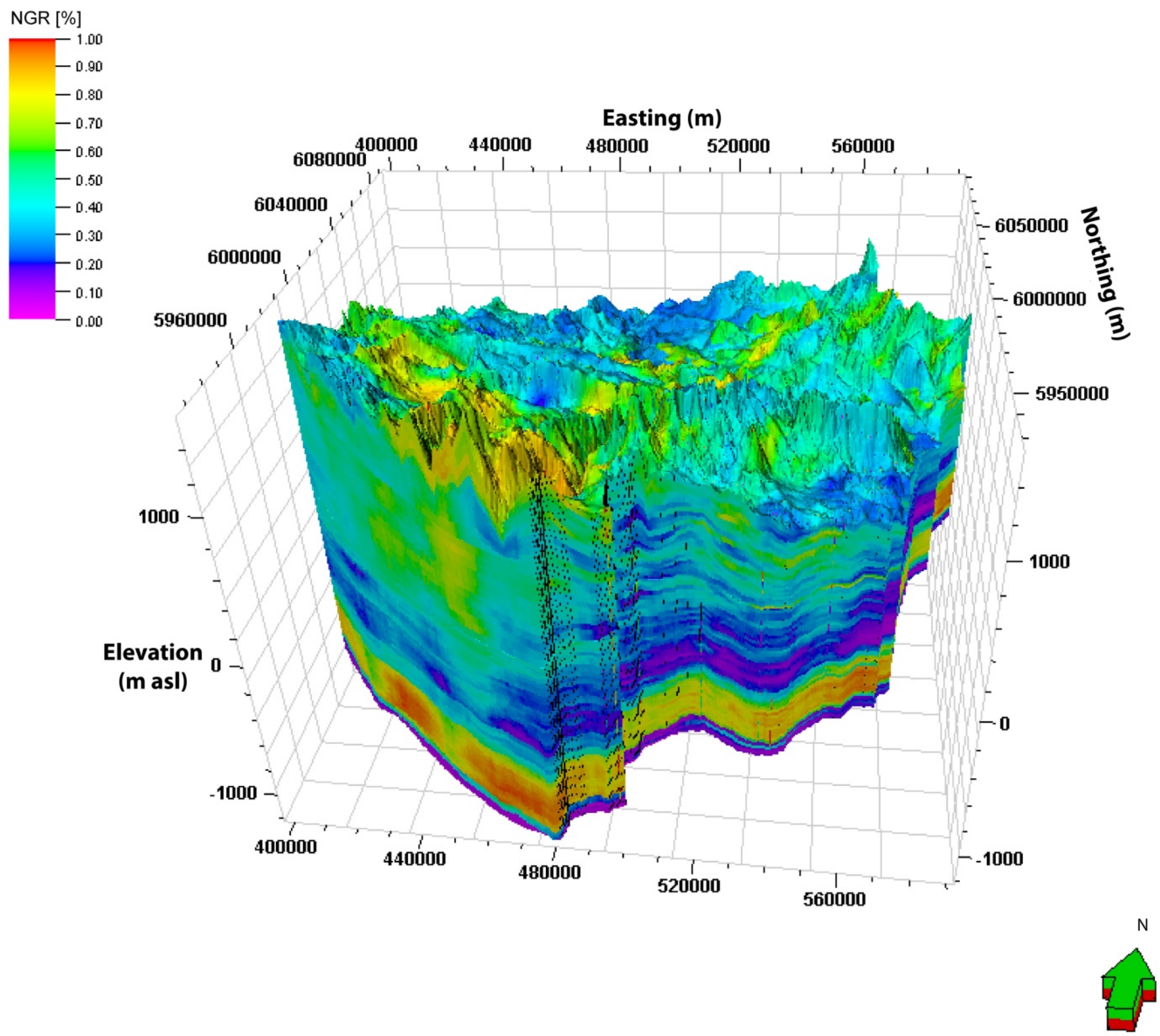

Figure 8. Assembled three-dimensional (3D) model of net-to-gross ratio (NGR) values, from the First White Speckled Shale unit of the Wapiabi Formation to the bedrock surface.

3 Model Quality

The 3D property model developed in this study is a rendering of sandstone abundance for a part of the subsurface in Alberta that is 22 170 km^2 in area and up to about 1800 m in depth. The model was developed from two different types of borehole data, each having a nonuniform distribution and data density. The quality of the 3D property model is dependent on the uncertainty of the input data and decisions made during analysis and modelling. Section 2.1 describes some of the typical sources of error associated with the input data. The approach of using slice mapping to generate a point-cloud dataset increased the uncertainty because the borehole log data was averaged over a larger volume (i.e., the slice interval) prior to 3D modelling. Thus, a limitation of the 3D property model will be an inaccurate representation of sandstone abundance at a spatial scale finer than the subsurface slices. The 3D property model developed for this study is appropriate only for regional-scale use (1:100 000). This model is not intended to be used in place of site-specific investigations because its accuracy is constrained by the data quality, quantity, distribution, and geological complexity at that scale.

4 Interpretation of Model Results

The 3D property model (Figure 8) illustrates a wide variation in sandstone abundance of geological formations in the study area. Zones having a high NGR value are likely to be more transmissive for water than surrounding sediments, and the spatial distribution of these zones establishes a basis to define the internal architecture of individual formations. Several regional trends are apparent from the model:

- a nearly continuous and approximately 230 m thick sandstone-dominated unit in the basal portion of the otherwise undifferentiated Wapiti Formation,
- a slightly discontinuous and approximately 200 m thick mudstone/shale unit within the middle portion of the undifferentiated Wapiti Formation,
- the absence of a basal sandstone-dominated unit within the Paskapoo Formation initially proposed by Lyster and Andriashek (2012),
- sandstone abundance in the uppermost portion of the Paskapoo Formation, and
- the dominance of NGR values of about 0.4 for the majority of the bedrock.

The lowermost part of the 3D property model represents the Lea Park Formation, which consists largely of mudstone having average NGR values of 0.12 and 0.39 for the lower and upper portions, respectively. Similar to other formations of the upper part of the underlying Colorado Group, this widespread fine-grained unit acts as a regional confining layer (Michael and Bachu, 2001).

The Wapiti Formation is a fluvial and floodplain deposit, with localized lacustrine sediments. Although the Wapiti Formation is undifferentiated in the study area, Dawson et al. (1994) described a lower unit consisting of medium-grained sandstone and siltstone and an absence of coal, and an upper unit consisting of interbedded fine-grained sandstone and mudstone with extensive coal seams. Fanti and Catuneanu (2009) suggested that the Wapiti Formation may have five distinct stratigraphic units corresponding to significant changes in major drainage systems during the Cretaceous. The results of 3D property modelling confirm that distinct stratigraphic units exist, with five submodels being used to estimate sandstone abundance in the Wapiti Formation. From a hydrogeological perspective, the nearly continuous and approximately 230 m thick basal sandstone unit with an average NGR value of 0.86 represents a potentially significant aquifer. Sandstone abundance decreases above this basal unit to an approximately 200 m thick mudstone/shale unit having an average NGR value of 0.23 within the middle portion of the Wapiti Formation. The uppermost portion of the Wapiti Formation appears to have subunits with average NGR values >0.30, indicating the potential for discontinuous sandstone units (e.g., channels) deposited within a floodplain environment. Upper portions of the Wapiti Formation also form the uppermost bedrock unit across the northern part of the study area, where some of the sandstone units are exposed as sections along rivers (Figure 9).

Overlying the Wapiti Formation is the discontinuous and relatively thin (<18 m thick) Battle Formation, which is mudstone-dominated (Hathway, 2011a, b). The average NGR value for the Battle Formation is 0.32, and it is generally considered as a discontinuous aquitard. In places, the Battle Formation has been locally removed by erosion that predated deposition of the Scollard Formation, so in places the overlying Scollard Formation is in direct contact with the underlying Wapiti Formation.

The Scollard Formation covers a large portion of the study area, and is the uppermost bedrock unit in a small section. It consists largely of sandstone and siltstone, interbedded with mudstone (Dawson et al., 1994). The upper portion of the Scollard Formation contains extensive coal seams, which distinguish the boundary with the overlying Paskapoo Formation. The Scollard Formation has an average NGR value of 0.42 and is considered to be heterogeneous, with localized sandstone units contained within siltstone and mudstone.

Figure 9. Outcrop of sandstone from the upper portion of the Wapiti Formation along the Simonette River, northwest of Fox Creek, Alberta.

The Paskapoo Formation is the uppermost bedrock unit across the southern half of the study area. It is dominated by siltstone and mudstone and interbedded with high permeability coarse-grained channel sandstone (Hamblin, 2004; Grasby et al., 2008). The 3D property model confirms the widely accepted view of the Paskapoo Formation being highly heterogeneous. The Paskapoo Formation has been divided into three members by Demchuk and Hills (1991): the Haynes, Lacombe, and Dalehurst members. Further division of the Paskapoo Formation has been made based on the occurrence of sandstones, resulting in three informal hydrostratigraphic units suggested by Lyster and Andriashek (2012): the Haynes and Sunchild aquifers and the Lacombe aquitard. The Haynes aquifer and Lacombe aquitard units correlate to the Haynes and Lacombe members, respectively, as proposed by Demchuk and Hills (1991). The Sunchild aquifer is suggested to be correlative to the Dalehurst Member and is characterized by permeable sandstone units that display variable interconnectivity due to incision by present-day streams (Lyster and Andriashek, 2012). The average NGR value for the Paskapoo Formation is 0.50, confirming greater abundance of sandstone units compared to the underlying Scollard Formation. The 3D property modelling confirms the presence of abundant sandstone in the uppermost part of the Paskapoo Formation (i.e., Sunchild aquifer) in the southwestern part of the study area, which is often exposed along the Athabasca River (Figure 10). The 3D property modelling also confirms the findings of Quartero et al. (2015), who suggested the absence of an extensive and thick basal sandstone unit (i.e., Haynes aquifer) in the study area.

Figure 10. Outcrop of sandstone from the Paskapoo Formation along the Athabasca River, south of Fox Creek, Alberta.

The 3D property model of the study area illustrates the high degree of heterogeneity of sandstone within these bedrock units. The 3D property model provides insight into the vertical and lateral connectivity of sandstone units and the degree of confinement (or compartmentalization) of the surrounding mudstone. Knowledge of sandstone unit geometry is useful for identifying aquifers, the extent of hydrogeological pathways, and also offers a line of evidence for future efforts in subdividing the undifferentiated Wapiti Formation quantitatively.

The 3D property model can be used to conceptualize the hydrostratigraphy, assuming that NGR values are a proxy for hydraulic properties such as porosity or permeability. These 3D data can help facilitate zonation of hydraulic properties directly within a numerical model of groundwater flow (e.g., Liggett and Singh, 2018), or provide a basis to develop hydrostratigraphy at a spatial scale that is fit for a specific purpose. Results of 3D property modelling can help inform hydrostratigraphic conceptualization that might be at a finer resolution than formation-scale geological mapping, but coarser than the actual 3D property model grid. A conceptual model of hydrostratigraphy developed from 3D property modelling allows definition of aquifers and aquitards within a single geological formation (Figure 11), which helps to better understand the components of a groundwater flow system. For example, Figure 11 depicts the thick aquitard and aquifer in the lower part of the Wapiti Formation, which would be unknown from formation level information.

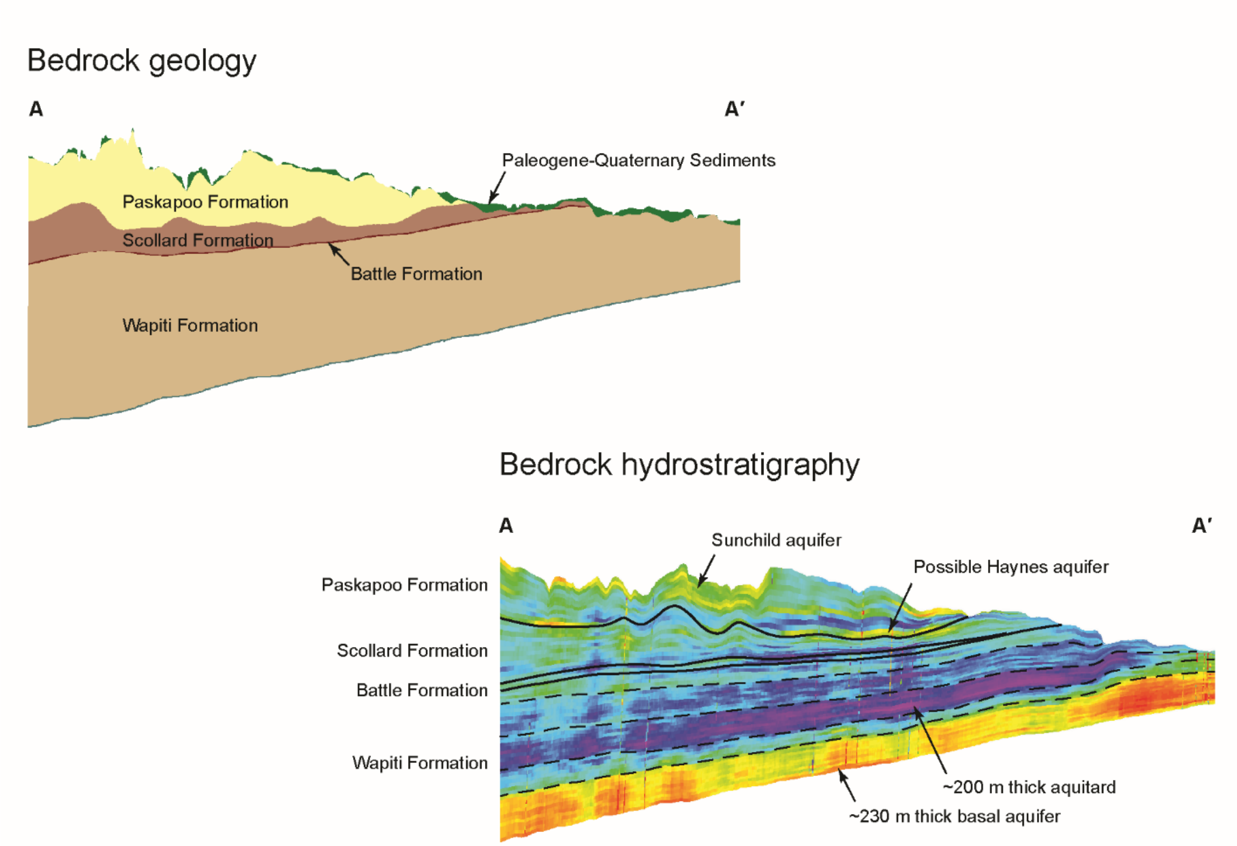

Figure 11. Hydrostratigraphic conceptualization of the bedrock deposits in the Fox Creek area (cross-section A–A′, location shown in Figure 1), illustrating permeable zones within the Paskapoo and Wapiti formations.

5 Summary

The 3D property model of the bedrock hydrostratigraphy provides a regional-scale (1:100 000) rendering of sandstone abundance for the region centred on the Town of Fox Creek, Alberta. The model includes the Lea Park, Wapiti, Battle, Scollard, and Paskapoo formations, and was developed from a combination of data sourced from gamma-ray logs from oil and gas wells and lithological descriptions from water wells. The 3D property model illustrates a wide range in sandstone abundance, where zones having a high NGR are likely to be aquifers within the surrounding siltstone–mudstone sedimentary rocks. The geometry of sandstone units has important implications for groundwater resources in this region, as well as providing insight to the depositional environment of the formations within which they are contained.

6 References

Alberta Energy Regulator (2019): Water use report; URL <https://www2.aer.ca/t/Production/views/AlbertaWaterUseReport_0/WaterSummary?:embed=y&:display_count=no&:showShareOptions=true&:showVizHome=no> [March 2019].

Alberta Environment and Parks (2018): Alberta Water Well Information Database; URL <https://www.alberta.ca/alberta-water-well-information-database-overview.aspx> [March 2018].

Atkinson, L.A. and Hartman, G.M.D. (2017): 3D rendering of the regional stratigraphy of Paleogene-Quaternary sediments in west-central Alberta; Alberta Energy Regulator, AER/AGS Report 93, 44 p., URL <http://ags.aer.ca/document/REP/REP_93.pdf> [March 2019].

Atkinson, L.A., Liggett, J.E., Hartman, G., Nakevska, N., Mei, S., MacCormack, K.E. and Palombi, D. (2017): Regional geological and hydrogeological characterizations of the Calgary-Lethbridge Corridor in the South Saskatchewan regional planning area; Alberta Energy Regulator, AER/AGS Report 91, 175 p., URL <http://ags.aer.ca/document/REP/REP_91.pdf> [March 2019].

Babakhani, M. and MacCormack, K. (2019): 3D geological model of west-central Alberta – methodology and metadata; *in* 3D geological model of west-central Alberta, Alberta Energy Regulator / Alberta Geological Survey, AER/AGS Model 2019-03, 62 p.

Corlett, H.J., Playter, T.L., Babakhani, M., Hathway, B., Peterson, J.T. and MacCormack, K.E. (2019): Regional stratigraphic correlation and 3D geological modelling of west-central Alberta; Alberta Energy Regulator / Alberta Geological Survey, AER/AGS Open File Report 2019-04, 53 p.

Dawson, F.M., Kalkreuth, W.D. and Sweet, A.R. (1994): Stratigraphic and coal resource potential of the Upper Cretaceous to Tertiary strata of northwestern Alberta; Geological Survey of Canada, Bulletin 466, 67 p.

Demchuk, T.D. and Hills, L.V. (1991): A re-examination of the Paskapoo Formation in central Alberta Plains; the designation of three new members; Bulletin of Canadian Petroleum Geology, v. 39, no. 3, p. 270–282.

Elliott, R.H.J. (1960): Subsurface correlation of the Edmonton Formation; Journal of the Alberta Society of Petroleum Geologists, v. 8, p. 324–338.

Fanti, F. and Catuneanu, O. (2009): Stratigraphy of the Upper Cretaceous Wapiti Formation, west central Alberta, Canada; Canadian Journal of Earth Sciences, v. 46, no. 4, p. 263–286, doi:10.1139/E09-020

Grasby, S.E., Chen, Z., Hamblin, A.O., Wozniak, P.R. and Sweet, A.R. (2008): Regional characterization of the Paskapoo bedrock aquifer system, southern Alberta; Canadian Journal of Earth Sciences, v. 45, no. 12, p. 1501–1516, doi:10.1139/E08-069

Hamblin, A.P. (2004): Paskapoo-Porcupine Hills formations in western Alberta: synthesis of regional geology and resource potential; Geological Survey of Canada, Open File 4679, 30 p.

Hathway, B. (2011a): Tops of the Horseshoe Canyon, Wapiti and Battle formations in the west central Alberta Plains: subsurface stratigraphic picks and modelled surface; Energy Resources Conservation Board, ERCB/AGS, Open File 2011-08, 24 p., URL <http://ags.aer.ca/publications/OFR_2011_08.html> [March 2019].

Hathway, B. (2011b): Late Maastrichtian paleovalley systems in west central Alberta: mapping the Battle Formation in the subsurface; Bulletin of Canadian Petroleum Geology, v. 59, no. 3, p. 195–206, doi:10.2113/gscpgbull.59.3.195

IHS Markit (2018): AccuMap™; IHS Markit, mapping, data management and analysis software, URL <https://ihsmarkit.com/products/oil-gas-tools-accumap.html> [March 2018].

Leckie, D.A., Battacharya, J.P., Bloch, J., Gilboy, C.F. and Norris, B. (1994): Cretaceous Colorado/Alberta Group of the Western Canada Sedimentary Basin; *in* Geological atlas of the Western Canada Sedimentary Basin, G.D. Mossop and I. Shetsen (comp.), Canadian Society of Petroleum Geologists and Alberta Research Council, URL <http://ags.aer.ca/reports/atlas-of-the-western-canada-sedimentary-basin.htm> [March 2019].

Liggett, J.E. and Singh, A. (2018): Numerical groundwater flow model of the Sylvan Lake sub-basin in the Edmonton–Calgary Corridor, central Alberta; Alberta Energy Regulator / Alberta Geological Survey, AER/AGS Report 96, 41 p., URL <https://ags.aer.ca/publications/REP_96.html> [March 2019].

Lyster, S. and Andriashek, L.D. (2012): Geostatistical rendering of the architecture of hydrostratigraphic units within the Paskapoo Formation, central Alberta; Energy Resources Conservation Board, ERCB/AGS Bulletin 66, 115 p., URL<http://ags.aer.ca/publications/BUL_066.html> [March 2019].

Mei, S. (2009): Geologist-controlled trend versus computer-controlled trend: introducing a high-resolution approach to subsurface structural mapping using well-log data, trend surface analysis and geospatial analysis; Canadian Journal of Earth Sciences, v. 46, p. 309–329, doi:10.1139/E09-024

Michael, K. and Bachu, S. (2001): Fluids and pressure distributions in the foreland-basin succession in the west-central part of the Alberta basin, Canada: evidence for permeability barriers and hydrocarbon generation and migration; American Association of Petroleum Geologists Bulletin, v. 85, no. 7, p. 1231–1252, URL <http://archives.datapages.com/data/bulletns/2001/07jul/1231/1231.htm> [March 2019].

Parks, K. and Andriashek, L. (2009): Preliminary investigation of potential, natural hydraulic pathways between the Scollard and Paskapoo formations in Alberta: implications for coalbed methane production; Energy Resources Conservation Board, ERCB/AGS Open File Report 2009-16, 66 p., URL <http://ags.aer.ca/publications/OFR_2009_16.html> [March 2019].

Prior, G.J., Hathway, B., Glombick, P.M., Pană, D.I., Banks, C.J., Hay, D.C., Schneider, C.L., Grobe, M., Elgr, R. and Weiss, J.A. (2013): Bedrock geology of Alberta; Alberta Energy Regulator, AER/AGS Map 600, scale 1:1 000 000, URL <http://ags.aer.ca/publications/MAP_600.html> [March 2019].

Quartero, E.M., Bechtel, D., Leier, A.L. and Bentley, L.R. (2014): Gamma-ray normalization of shallow well-log data with applications to the Paleocene Paskapoo Formation, Alberta; Canadian Journal of Earth Sciences, v. 51, no. 5, p. 452–465, doi:10.1139/cjes-2013-0148

Quartero, E.M., Leier, A.L., Bentley, L.R. and Glombick, P. (2015): Basin-scale stratigraphic architecture and potential Paleocene distributive fluvial systems of the Cordilleran Foreland Basin, Alberta, Canada; Sedimentary Geology, v. 316, p. 26–38, doi:10.1016/j.sedgeo.2014.11.005

Tyler, N. and Finley, R.J. (1991): Architectural controls on the recovery of hydrocarbons from sandstone reservoirs; *in* The three-dimensional facies architecture of terrigenous clastic sediments and its implications for hydrocarbon discovery and recovery, A.D. Miall and N. Tyler (ed.), Society for Sedimentary Geology, Concepts in Sedimentology and Paleontology, v. 3, p. 1–5.